Contact pressure distribution during the polishing process of ceramic tiles: A laboratory investigation

2016 IOP Conf. Ser.: Mater. Sci. Eng. 114 012008

(http://iopscience.iop.org/1757-899X/114/1/012008)

IOP Conf. Series: Materials Science and Engineering **114** (2016) 012008 doi:10.1088/1757-899X/114/1/012008

Contact pressure distribution during the polishing process of ceramic tiles: A laboratory investigation

A S A Sani[1,3], F J P Sousa[2], Z Hamedon[1] and A Azhari[1]

[1] Faculty of Manufacturing Engineering, Universiti Malaysia Pahang, 26600 Pekan, Pahang, Malaysia
[2] Institute for Manufacturing Engineering and Production Management, University of Kaiserslautern, POBox 3049, D-67653 Kaiserslautern, Germany

E-mail: asas2601@gmail.com, sousa@cpk.uni-kl.de, zamzuri@ump.edu.my, azmir@ump.edu.my

Abstract. During the polishing process of porcelain tiles the difference in scratching speed between innermost and peripheral abrasives leads to pressure gradients linearly distributed along the radial direction of the abrasive tool. The aim of this paper is to investigate such pressure gradient in laboratory scale. For this purpose polishing tests were performed on ceramic tiles according to the industrial practices using a custom-made CNC tribometer. Gradual wear on both abrasives and machined surface of the floor tile were measured. The experimental results suggested that the pressure gradient tends to cause an inclination of the abraded surfaces, which becomes stable after a given polishing period. In addition to the wear depth of the machined surface, the highest value of gloss and finest surface finish were observed at the lowest point of the worn out surface of the ceramic floor tile corresponding to the point of highest pressure and lowest scratching speed.

1. Introduction

Modern manufacturing processes have shown the importance of surface finish in various fields of current technology. According to literature [1] surface finish of ceramic tiles can be achieved by grinding, honing, lapping and polishing, under the same standard of machining of geometrical indefinite cutting edges. The basic differences between these processes are the number and the type of contacts happening between the abrasive particles and the abraded surfaces in a period of time [2].

The surface finish of porcelain ceramic tile has made them an excellent choice for a wide variety of applications in architecture. The good mechanical strength as well as abrasion, chemical, stains and frost resistances are often mentioned as the main attractive properties of highly polished unglazed porcelain ceramic tiles [3 – 7].

In the industries the polishing process is accomplished by rotatory tangential polishing heads, using abrasive blocks, called fickerts, as abrasive tool [3, 8]. The difference of scratching speed between the innermost and the peripheral abrasive particle during the rotation of the fickerts causes a linear variation of the normal pressure along the contact surface between the fickerts and the surface being polished [8]. The resulting pressure gradient was investigated elsewhere [9 – 10]. The basic idea of

[3] To whom any correspondence should be addressed.

this work is to extend those investigations using a custom made CNC tribometer, which was built in laboratory scales to match the industrial ceramic polishing processes [11].

Recent developments in the field of polishing ceramic tiles [8, 11-12] have led to a renewed interest in optimizing the surface pressure distribution produced during the contact between surfaces of ceramic tile and polishing head, thus requiring a good understanding of the wear evolution during the polishing process. The main goal of the present work is to assess the correlations between surface topography, wear, and glossiness promoted by the polishing process of porcelain tiles, under a controlled condition of pressure gradients. These information might contribute not only to improve the total cost of manufacturing ceramic tiles but also to the reduction of waste and defected final products [6, 12].

2. Pressure gradient analysis

The distribution of contact pressure beneath the polishing head can be explained considering a motion diagram in equilibrium. The first mathematical approach is to describe the equation of motion of an abrasive block subjected to a loading that is linearly distributed over its surface. In the presence of hypothetical helical springs acting against any rotation of the abrasive block, the distributed-loading diagram can be illustrated as in figure 1.

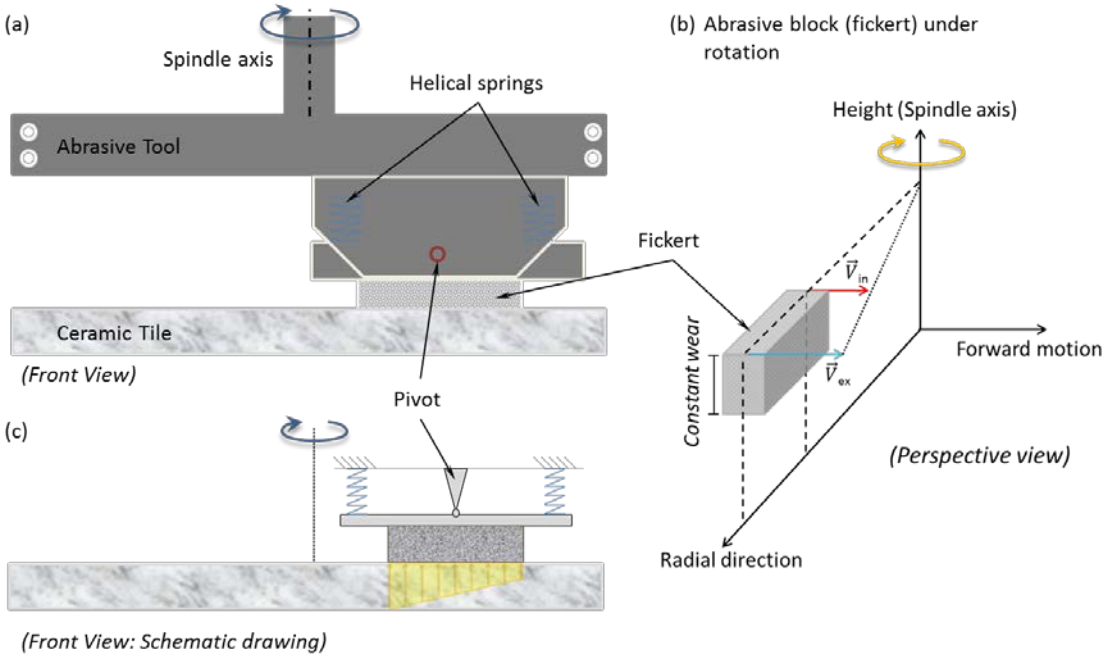

Figure 1. Polishing head (a) in front view, (b) the schematic diagram and (c) the perspective view of the abrasive block moving during the polishing process.

If the abrasive tool is set to work at the same position on the tile surface, the presence of such radial pressure gradient leads to inclined wear profiles on both the abrasive tool and on the tile surface. This resulting inclination α can be experimentally measured by coordinate measuring system. Since this study was conducted using two identical helical springs to impose a controlled rotation resistance of the abrasive tool, the pressure gradient could be mathematically determined by analyzing the relationship between the inclination α and the stiffness of the springs. The springs were placed in a distance of 100 mm apart to each other, and centered with the abrasive block. The force acts along the line which intersects the pivot joint. At the same time, the moment resulting from the pressure gradient is balanced by the springs.

The grinding tools, or fickerts, move and rotate around the centre of the polishing head [8]. The kinematics behind those motions was studied elsewhere [9] to demonstrate the mathematical equations which deal with the displacement vectors and power per unit time performed by polishing work. Such investigations revealed by computer simulation [9] suggest that the contact pressure tends to be 50% higher near to the centre, in regions worked by the innermost abrasives.

In 2004, Cantavella et al. [8] published a paper in which the genesis of the pressure gradient is described. The work performed by grinding tools at different points of porcelain tile surfaces is given by equation (1). The work executed by the polishing tools was basically divided into three main subjects which are the tool abrasion, the polishing process and other influence factors which contribute mainly to the tribological interactions between fickert and ceramic tile. The proposed model was later combined with the kinematics equations of a single rotating abrasive particle with lateral and traversal motions into computational simulation [13].

$$d\dot{W} = \omega \cdot r \cdot \mu \cdot p \cdot dA \tag{1}$$

where:

p is the contact pressure in N/mm^2;
ω is the angular speed of the polishing head in rad/s;
r is the distance from the centre of the polishing head to the fickert element in mm;
μ is the coefficient of friction between the abrasive block and the tile surface;
dA is the contact surface between fickert and tile in mm^2.

With the rotation motion of the polishing head, a linear variation of velocity along the radius was demonstrated therein. Cantavella et al. also performed computer simulations in their work. Their basic assumption was that, if the abrasive block is always moving and working on different parts of the tile surface, the fickerts are supposed to abrade equally during the polishing work [8]. Therefore, both abrasive blocks and tiles tend to remain flat during the polishing process. On the other hand, the work done per unit time, as suggested by equation (1) varies directly with the radius, *r*. The outer particle underwent longer distance than the particle near to the rotation axis. The equation of distance travelled, *s* with its corresponding speed, v_r is given by equations (2) and (3) respectively.

$$ds = dv_r \cdot dt \tag{2}$$

$$v_r = \omega \cdot r \tag{3}$$

As a consequence, even under a constant normal load, radially oriented gradient of pressure will take place. The loading diagram in figure 2 shows the mechanics of grinding process during the rotation of the tools. A better visualization of the loading diagram and the after effect of surface wear of both work piece and tools can be obtained by analyzing a single abrasive tool. The polishing tool is pressed downwards. Both springs' displacements are equidistant and in different direction. The compression of the spring resulted in more pressure exerted against the tile surface. Consequently, when the tool is set to remain working at the same place, higher wear rates on near to the tile centre might be expected in both ceramic tile and abrasive block, since it is there where the maximum normal pressure is located. The force moment about the pivot joint can be determined by considering all forces acting in the system. The distributed loads on the grinding tools can be calculated with a diagram of motion in static state.

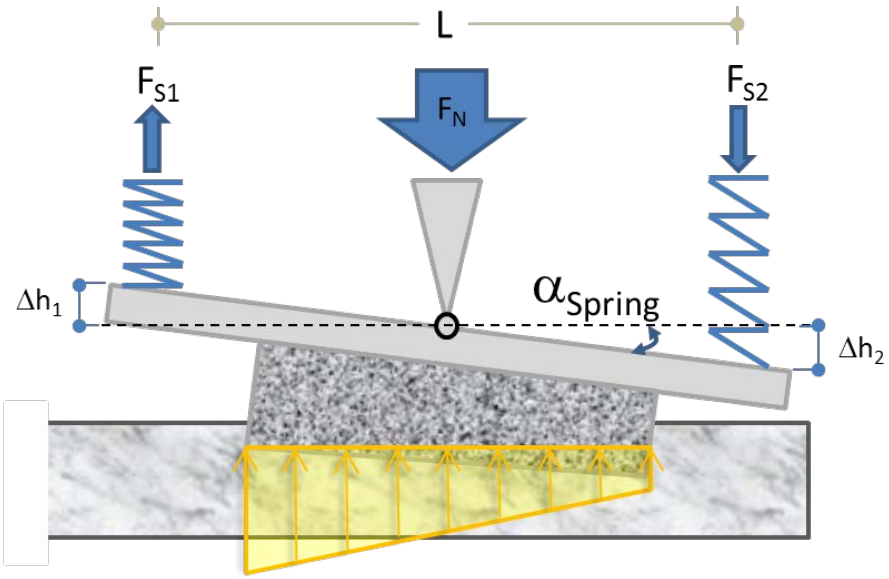

Figure 2. Loading diagram of the polishing tool and the abraded tile's surface.

For the purpose of determining the force moment around the hinge joint, the displacements of the springs and the resultant forces were highlighted in figure 2, where the inclination α_{spring} represents the rotation caused of the moments acting on the joint. Thus, the deformation suffered by the springs can be put into a mathematical equation as below:

$$\Delta h_1 = -\Delta h_2 = \Delta h \tag{4}$$

The two opposing forces, $F_{S1} = -F_{S2}$, were applied equidistant from the hinge joint and named as the springs' resultant force, F_{Spring} .This force resists the rotation motion of the tool's holder around the hinge joint, causing a moment force, M_{Spring} , around the pivot joint. Therefore, the arctangent of the inclination angle is the product of the geometrical changes as shown in figure 2 and can be given as:

$$\alpha_{Spring} = \arctan\left(\frac{2 \cdot \Delta h}{L}\right) \tag{5}$$

L is the distance between the centre of both springs and Δh is the distance moved by compression or extension of the springs. The inclination angle, α_{spring} , is very small in relation to the geometrical changes. The values experimentally measured were always smaller than 1°. Hence, the deformation of the spring can be expressed with the geometrical changes of the abraded surfaces alone.

$$\Delta h \approx \frac{\alpha_{Spring} \cdot L}{2} \tag{6}$$

The equation of a linear spring under stress is given by Hooke's law, where the force, F_{spring} needed to extend or compress a spring by its displacement, Δh is proportional to that distance. The stiffness factor characteristic to the helical spring, c_{spring} , is equal to 20.25 N/mm according to the manufacturer Febrotec Federn (P/N: 0C0480-0811250S) [14].

$$F_{Spring} = c_{Spring} \cdot \Delta h \tag{7}$$

Finally the tendency of the tool's holder to move around the hinge joint is then given by the product of the resultant force and the proportional distance to the force.

$$M_{Spring} = F_{Spring} \cdot L \tag{8}$$

By rearranging equations (6) and (7) into equation (8), the moment force of the springs around the hinge joint is expressed by the following equation:

$$M_{Spring} = \frac{\alpha_{Spring} \cdot c_{Spring} \cdot L^2}{2} \tag{9}$$

Equation (9) expresses the rotation moment, M_{spring} , provided by the springs as a function of the inclination angle, α_{spring}, the spring stiffness, c_{spring} , and the distance between the springs, L. The unknown variable in this equation, α_{spring} , can be derived by measuring the abraded surfaces of both grinding tool and work piece. Figure 3 depicts the relationship between both inclined surfaces of the abrasive and the machined surface of the ceramic tile. Both inclined surfaces are considered as the result of the spring displacement due to material removal during polishing process. The relation between both inclined surfaces can be equated as $\alpha_{spring} = \alpha_{Tile} + \alpha_{Abrasive}$.

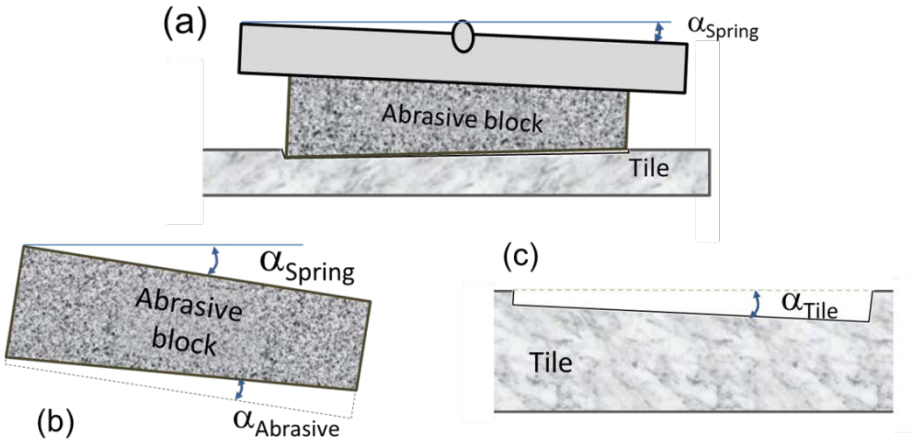

Figure 3. (a) Total inclination angle of the spring composed by inclination caused by (b) the wear of the abrasive block and by (c) the wear of the ceramic tile.

The information above will be used to develop the equation of spring pressure distribution beneath and across the abrasive surface. It is necessary here to clarify the effective distribution of load acting on the machined surface of the ceramic tile by the abrasive pressure. Figure 4 shows the abrasive length, L_{abr} , the loading diagram and its loading equivalence.

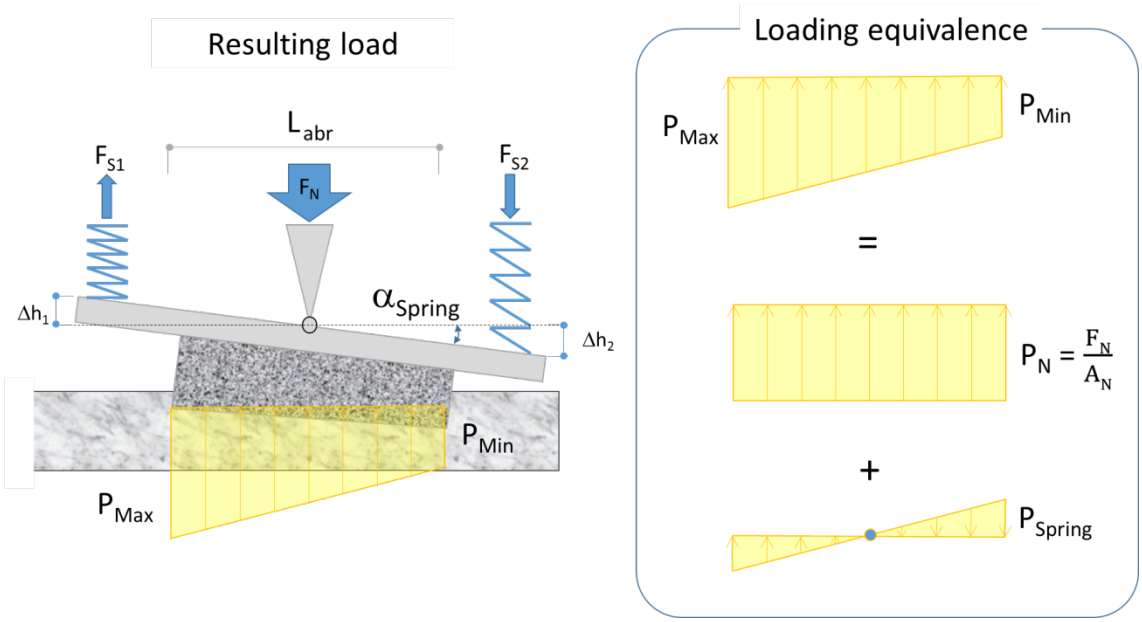

Figure 4. Loading diagram of the abrasive block in 2D and its equivalence.

The pressure loading is assumed to vary only along the horizontal plane parallel to the tile surface. The volume of the loading diagram (here: trapezoid) is equal to the resultant normal force acting on the grinding tool. The loading equivalence may also be defined as the resultant surface pressure of two loading diagrams overlapping each other to define the maximum and minimum gradient of pressure distribution, as seen in figure 5.

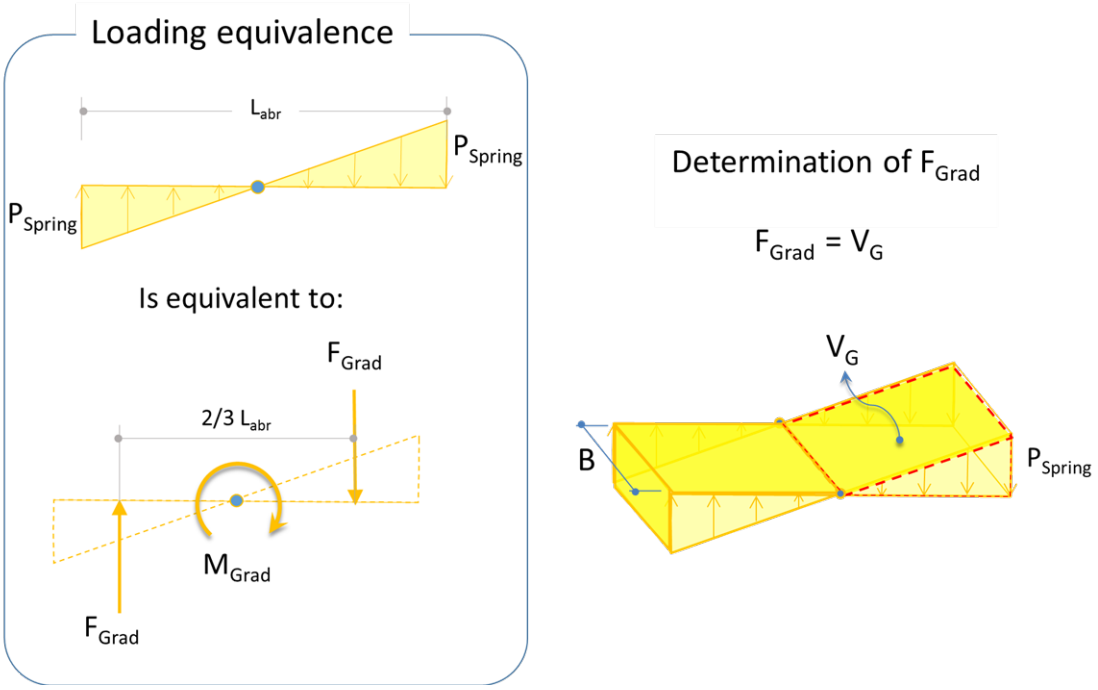

Figure 5. Loading diagram exerted by the helical springs; Right: Surface load in 3D.

The maximum pressure, P_{Max} and the minimum pressure, P_{Min} can then be expressed as the summation of the spring pressure, P_{Spring}, which has the same magnitude but in different direction. The

unknown variable P_{Spring} could be determined by solving the equation of force and depicted in figures 4 and 5. The minimum and maximum pressures exerted by the helical springs are:

$$P_{Max} = P_N + P_{Spring}$$
$$P_{Min} = P_N - P_{Spring} \quad (10)$$

To determine the magnitude of the spring pressure, P_{Spring}, it is necessary to define the volume of the surface pressure, V_G into an equivalent line load, F_{Grad}. The equivalent line load is acting at the centroid of the triangular load shape which is 1/3 of the height from the base as illustrated in figure 5. The magnitude of the defined line load, F_{Grad} is equal to the volume of a right triangular prism, V_G. Henceforth, the equivalent line load could be established by considering the volume of the force diagram and may be defined as below:

$$F_{Grad} = \frac{P_{Spring} \cdot B \cdot L_{abr}}{4} \quad (11)$$

The force moment, M_{Grad} , around the hinge joint by the line load, F_{Grad} as a function of spring pressure, P_{Spring} must be considered. It is equal to the vector product of the gradient force and its proportional distance and is given as:

$$M_{Grad} = \frac{P_{Spring} \cdot B \cdot L_{abr}^{\ 2}}{6} \quad (12)$$

The line loads illustrated in figure 6 are the resultant forces against the spring pressure acting on the abrasive block during the polishing process. The force moment caused by the springs and the pressure distribution across the fickerts at the hinge joint, are equal in the state of equilibrium.

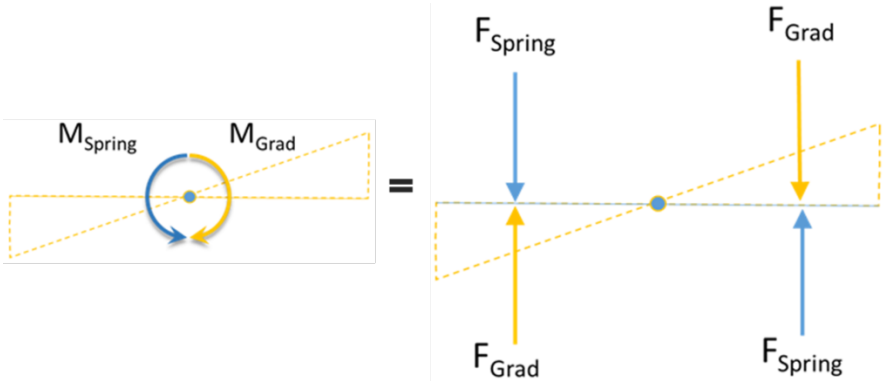

Figure 6. Moments at pivot joint; Right: Resultant forces acting on the abrasive block due to spring pressure.

$$P_{Spring} = 3 \cdot \frac{\alpha_{Spring} \cdot c_{Spring}}{B \cdot} \cdot \frac{L^2}{L_{abr}^{\ 2}} \quad (13)$$

It can be noted from equation (13) that the absorbed pressure by the springs varies with the geometrical ratio between the distance of two helical springs and the length of the abrasive block raised to the power of two. Finally, rearranging equations (13) into (10), one may also conclude that the pressure is distributed gradually along the abraded surfaces of the grinding tools.

3. Experimental work

All polishing tests were performed with the contact region flooded with tap water, like used elsewhere [15], which was neutral with a pH scale of approximately 7, as the lubricating coolant. The water flow was set to be constant at 1 liter/min and was electronically controlled during all the polishing work.

All abrasive blocks (or fickerts) used in this work were produced by Abrasivi Theobald from St. Ingbert, Germany. They are commercially found in European ceramic polishing industries. The abrasive particles are made from silicon carbide and embedded in magnesium oxychloride cement matrix. The finest grain size, #Lux on the other hand, is resin bonded abrasive particles [11-12]. They were cut down into segments of 60 mm length by 10 mm width and approximately 24 mm height. These segments were bonded onto the holder using hot melted polymer as adhesive material. At next, the abrasive block fixed on the holder was fastened to the tribometer for dressing. The abrasive was dressed in a way that a flat surface perpendicular to the rotating axis was achieved. The surface topography of the abrasive was then measured with CMM. The initial value of inclination angle, height of the abrasive and radius were taken for initial data tabulation. The abrasive holder was fixed on the polishing head with two helical springs in between. The experimental parameters used in this work are given in table 1. These parameters are kept constant in order to produce constant load distribution underneath the fickerts surface and to investigate the effect of the calibrated springs on the formation of pressure gradient during the polishing operation of ceramic tiles.

Table 1. Parameter that were kept constant during all polishing processes.

RPM in min^{-1}	Normal load, F_N in N	Angle of contact	Abrasive length in mm	Abrasive width in mm	Spring constant in N/mm	Linear load in N/mm	Maximum contact pressure in MPa
120	102	0°	60	10	20.25	1.7	0.17

According to Hutchings [6, 15], the linear load adopted in this work was the same that typically used in industry. However, due to the impossibility of using a condition of linear contact between the abrasive block and the tile surface, a maximum contact pressure that was 100 times smaller than that found in industries was implemented.

Previous laboratorial tests revealed that under such very small contact pressure the consumption of the abrasive blocks requires several days to become significant. For this reason, two different experimental approaches were used in this work. The first approach was intended to accelerate the wear process of the abrasive blocks, as well as to prepare the fickert surface for the second approach. However, by monitoring the inclination angle during this first approach, the time required for the stabilization of the wear could also be achieved. The second approach effectively uses the abrasive blocks prepared by the first approach to investigate the development of glossiness.

For each one of these two experiments a different kind of ceramic floor tile and polishing kinematics were used. The first kind was an ordinary commercial porcelain tile, whereas the second kind was the one of interest for further surface evaluations. The tile used for investigating the glossiness is a commercially available porcelain tile known as ‘Black-Onix’, produced by the Brazilian company Cecrisa S.A. These tiles were imported from Brazil to Germany in scope of a collaborative research work, therefore, due to the limited availability of the Brazilian tile, an ordinary porcelain tile was used for the first approach, in which only the fickert surface was of interest.

3.1. First experimental approach – Stabilization of the inclination angle

As previously mentioned, the main purpose of this first approach was to prepare the surface of the fickert for the second experimental setup. The original surface of the fickert is totally flat and has no slope angle ($\alpha_{Abrasive} = 0$). During the gradual consumption of the fickerts, the inclination $\alpha_{Abrasive}$ starts to increase due to the presence of the pressure gradient, described in detail in section 2. Such increase is however, limited by the resistance imposed by the helical springs. Therefore, by measuring the

inclination angle during the consumption of the fickert, it was possible to evaluate such stabilization process.

The abrasive blocks were polished against the common ceramic tile with an exponentially increased number of contacts in order to investigate the stationary value of the inclination angle. The experiment began with measuring the topography of the initial flat surface of every abrasive blocks. Dressing of the abrasive blocks was necessary, so that the first statistical measurement starts with a very flat contact area with initial inclination angle of zero.

The sample used in this first approach had width and length of ca. 270 mm and 300 mm, cut from an unpolished porcelain stoneware tile. It is commonly found in the European market under the commercial name 'Spazio' and was produced by MML, Malaysia. This sample was hereafter termed Sample 1 (S1), and was the same for the entire investigation.

The number of contacts occurred after each cycle was calculated according to the equation mentioned in previous work by Olenburg et al. [10]. The polishing kinematics used in this approach is illustrated in figure 7. It consists of clockwise rotation and traversal movement to maintain the linear wear gradient of the abrasive blocks. The abrasive blocks were polished against the common ceramic tile with an exponentially increased number of contacts and the presence of helical springs.

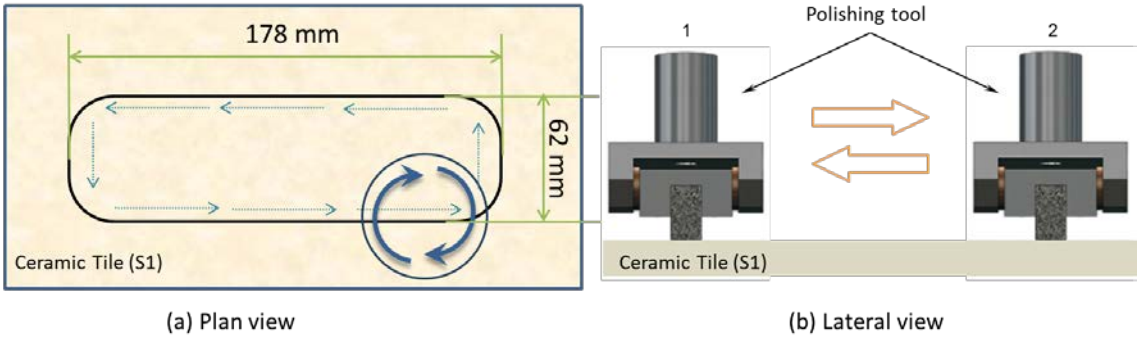

Figure 7. Kinematics of polishing process in first methodology.

The height of the abrasive block was measured with a coordinate measuring machine (CMM) with a grid size of 9x12 measuring points (refer section 3.3). The measurement's routine was programmed in advance. All data recorded by CMM were exported into a text-file data which can be manipulated using LabVIEW or Excel spreadsheet for further result analyses.

After getting the stationary value of the inclination angle, the grinded abrasive block was then used to carry out the second experimental approach described at next.

3.2. Second experimental approach – Rotation with pressure gradient

For this second approach, a commercially available porcelain tile, 'Black-Onix' from Cecrisa S.A., Brazil was cut into a square shape of 200 mm length by 200 mm wide with a default width of 9 mm. This sample was termed Sample 2 (S2). The glossy surface of the 'Black-Onix' was sandblasted in a shape of a ring. The dimension of the outer and inner diameter of the ring was 180 mm and 60 mm respectively. Through sandblasting process the plane topography was kept unaltered and the initial gloss is removed with minimum material loss. The rest of the tile surface was covered with adhesive tape (acting like a stencil) before the sandblasting process in order to keep the reference points for topography measurements. [11]

The kinematics was a simple rotation movement on the machined surface of the ceramic tile, as depicted in figure 8. The number of contacts differs from the first experimental approach and was calculated simply by multiplying the number of rotation per second with the duration of the polishing process. During this experiment, each polishing cycles of the fickert lasts for 250 seconds.

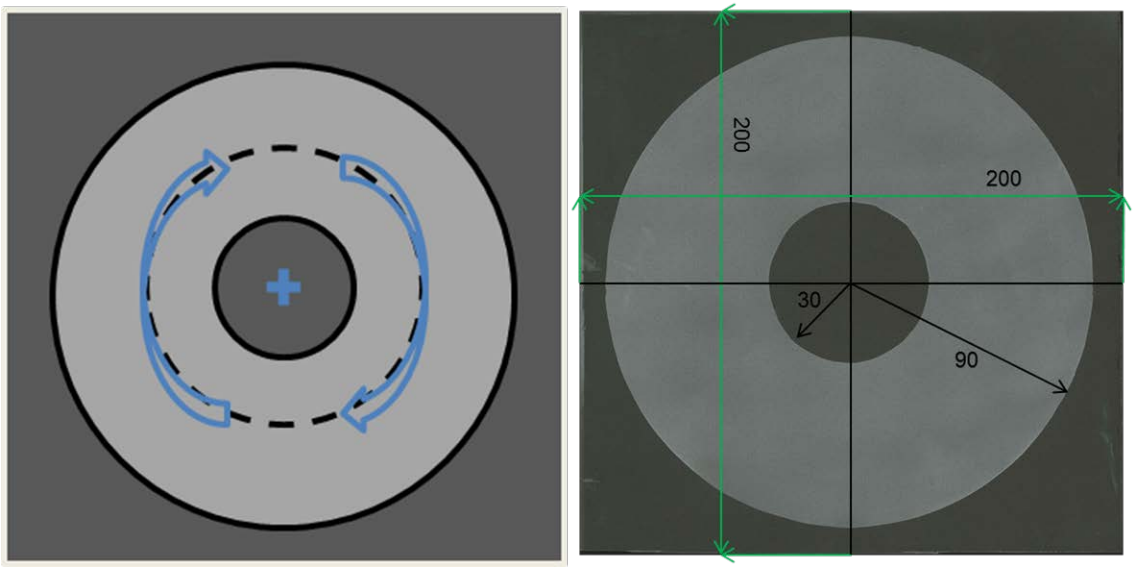

Figure 8. Kinematics of the polishing process in second experiment. Right: Sample of `Black Onix' tile with its sandblasted dimension.

The entire experimental cycle is illustrated in figure 9:

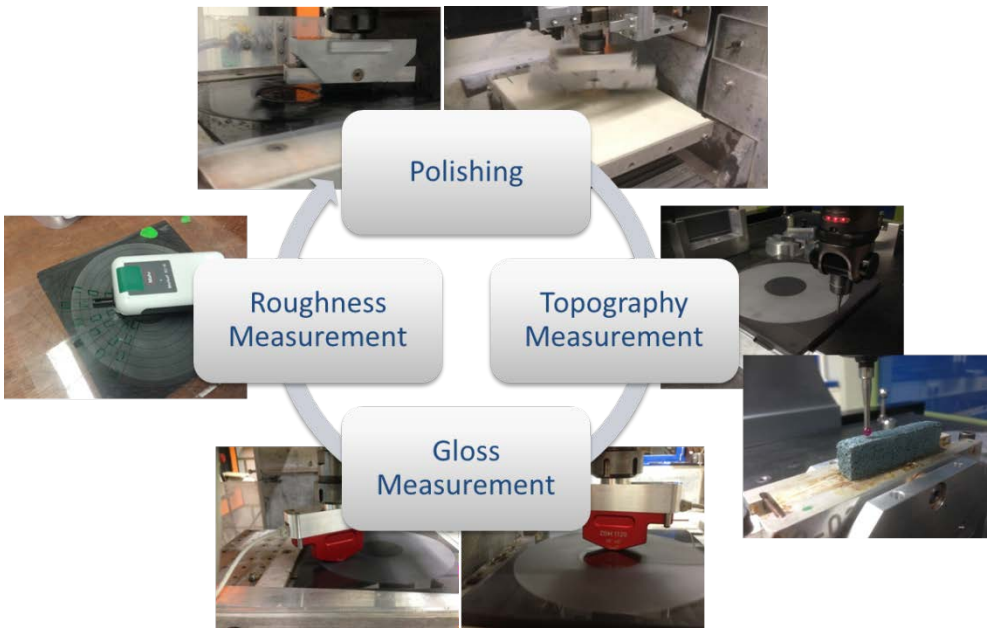

Figure 9. Experimental cycles.

3.3. Data acquisition

Firstly the topography of abrasive blocks and ceramic tile were determined along a grid of 9x12 and 8x36 measurement points respectively. In a row of 8 points, the distance between two points was set to 10 mm and the straight line was projected for 10° to form a complete circle. During this step, non-machined surfaces were also included as reference points, in order to allow posterior measurements of the removed material. 216 points inside the machined area were taken for the calculation of the thickness layer and removed material.

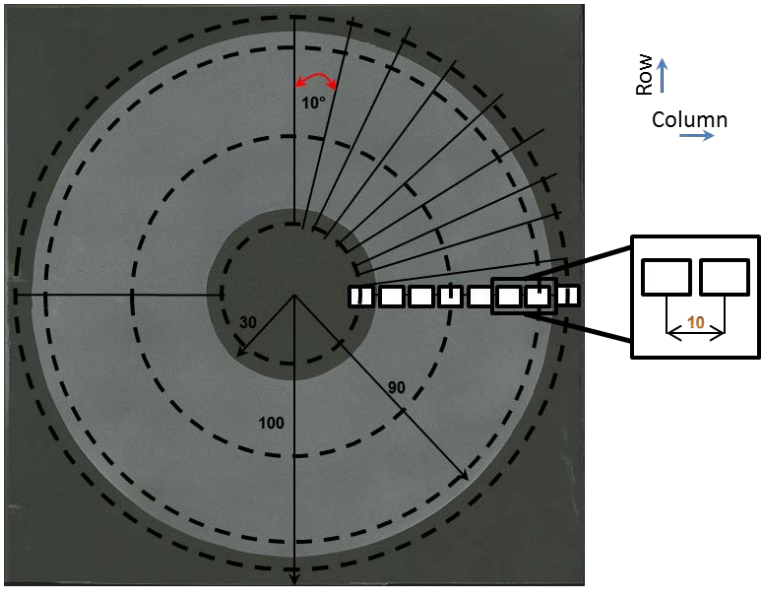

Figure 10. Measuring points of a ceramic tile sample with CMM.

The total measurement points on an abrasive block were 108 points. There were 12 points per columns and 9 points for every row in the measuring grid matrix. The distance between two points was set to 1 mm longitudinal by 5 mm lateral. The coordinate points are depicted in figure 11, where the length of the abrasive is equal to 60 mm.

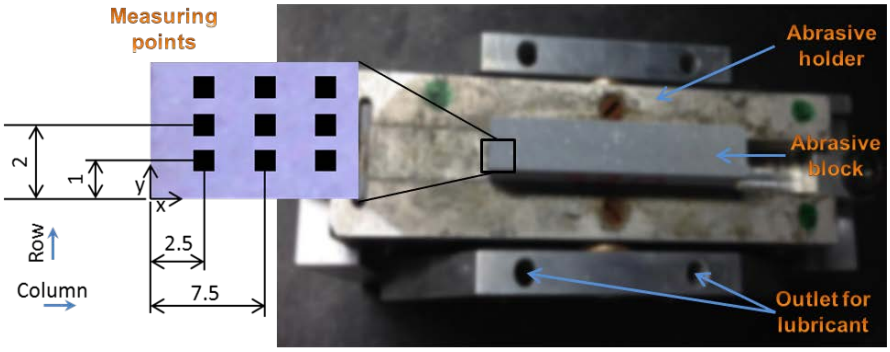

Figure 11. Measuring points of an abrasive block under CMM.

For glossiness level, the grid points were 6x9 on each one of the two regions shown in figure 12. The angle of incidence during measurement of gloss was 60° and the measurement was taken on the machined surface tangential to the scratching direction.

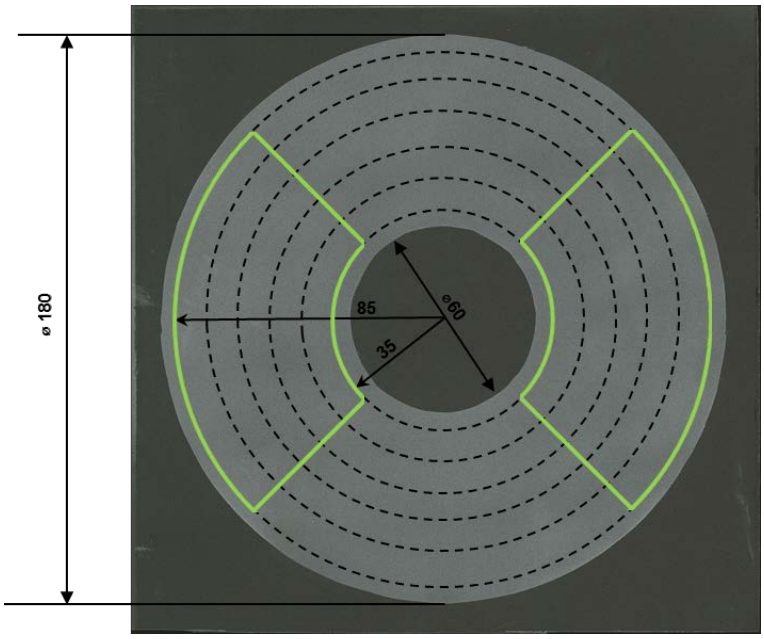

Figure 12. Area covered by the glossmeter during the measurement of gloss level.

The roughness was measured approximately on the same area used to measure the gloss level. The grid points were 3x6 measurement points. A figure with 8 columns projected 10° from one another was printed on a transparent stencil. Three rows were selected for each 6 columns as displayed in figure 13. The stencil was then used to cover the machined surface of the ceramic tile in order to provide approximately the same measuring points of surface roughness for each experiment.

The sequence of measuring the roughness at each measuring points started from the first segment at the top left. It continued to the right rows and finished column by column until all 18 points are measured. The measurement setting on the portable roughness measurement device MarSurf M 300 by Mahr was done according to DIN EN ISO 4288 where the sampling length is 0.8 mm and the total length for seven samplings is 5.6 mm.

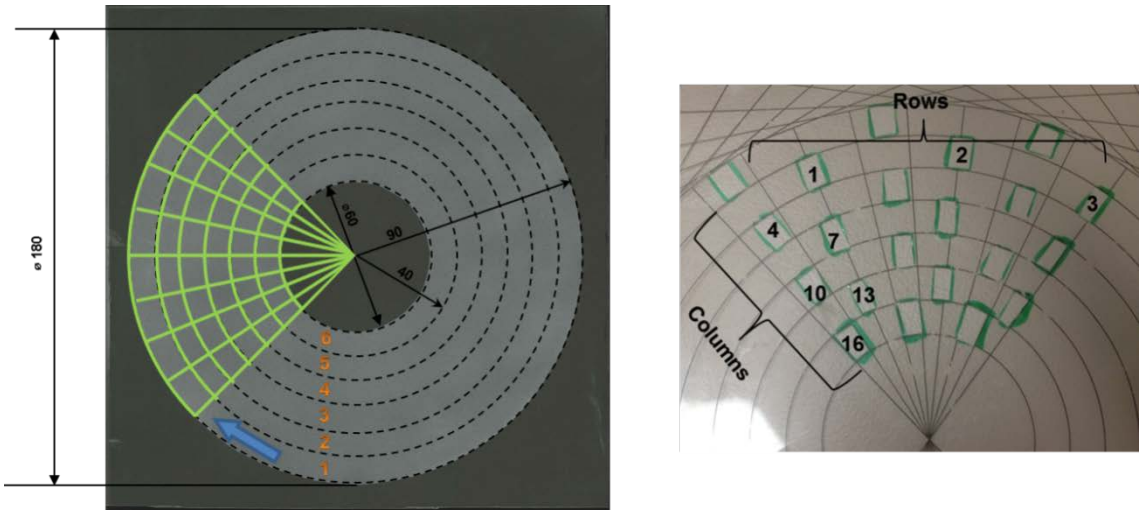

Figure 13. Illustration of the grid size on tile surface; Right: A transparent plastic stencil with the measurement sequence.

4. Results and Discussion

Results of the first experiment are presented in figure 14. The horizontal axis represents the height of the abraded abrasive block (removed material), representing the average wear during the polishing operation. During the removal of the first two millimeters, the inclination angle increases with the wear of the fickert, represented by its height variation. This means the tribological system was still under stabilization. As expected, after some time, which was different for each size of abrasive particles, the inclination $\alpha_{Abrasive}$ reaches a stationary regime due to the presence of the helical springs. An issue that must be taken into consideration is that different removal rates were found for each abrasive size. All tests were set to stop either after about 13800 abrasive contacts or by an excessive consumption of the abrasive blocks (ca. 8 mm). Table 2 depicts the total amount of material removed from the abrasive blocks used and the total number of contacts reached during the experiments for each abrasive.

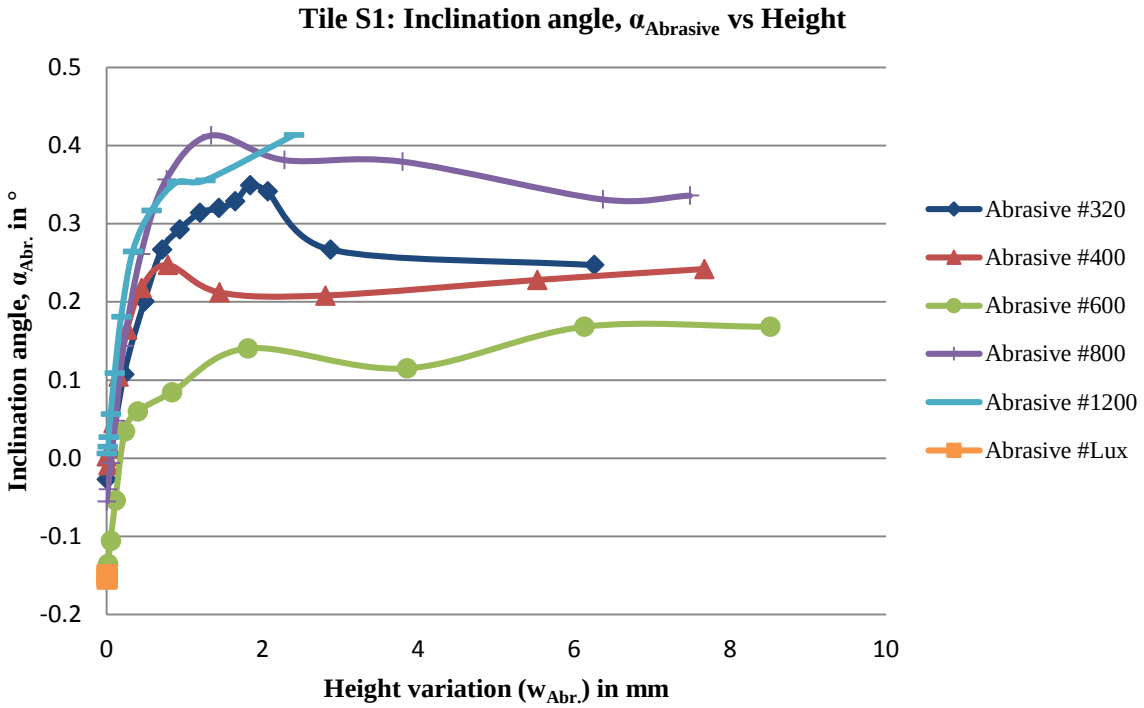

Figure 14. Evolution of inclination angle and its height of an abraded abrasive blocks from #320 until #Lux.

It is apparent from table 2 that the abrasive block with mesh number of 600 abraded much faster than all others, which could explain the different general behavior of its stabilization curve. On the contrary, due to the extreme small removal rates found for the two finest abrasive blocks, their corresponding stabilization curves could not be totally achieved during the period stipulated for the tests. The reason for this could be the very fine texture left by all the previous contacts from the coarser abrasive blocks on the ceramic stoneware tile, S1. The angles given in table 2 are the final averaged value after all the polishing tests. Figure 14 still reveals that for the tribological system used in this work, the inclination angle $\alpha_{Abrasive}$ asymptotically tends toward a value of ca. 0.25 degree, and that the coarser the abrasive particles, the faster is the stabilization process. As discussed in section 2, this limiting value results directly from the equilibrium between the action of the helical springs and the pressure gradient generated by difference of scratching speed between innermost and peripheral abrasives of the fickerts.

Table 2. Data of polishing Sample 1

Mesh number	Number of Contact	Angle, $\alpha_{Abrasive}$ in °	Removed material in mm
#320	13815	0.247040	6.254
#400	12683	0.241873	7.668
#600	4599	0.168168	8.512
#800	11265	0.336108	7.483
#1200	13815	0.413295	2.402
#Lux	13815	-0.149193	0.01

From the theory of pressure distribution mentioned in section 2, the distributed pressure acting across the abrasive surface is influenced by the stiffness of the helical springs. Torque is produced by the two springs across the pivot joint of the abrasive holder and therefore concentrating the pressure more towards the side where the spring is compressed, while the other spring is elongated during the polishing process. A scatter diagram and the mathematical equations developed in section 2 were used to determine the relationship between spring pressure and the inclination angles measured by CMM. By calculating the displacement of springs from the inclination angle, the magnitude of the toruqe acting across the abrasive surface as a function of inclination angle could be given by equation (9). The result is shown in figure 15.

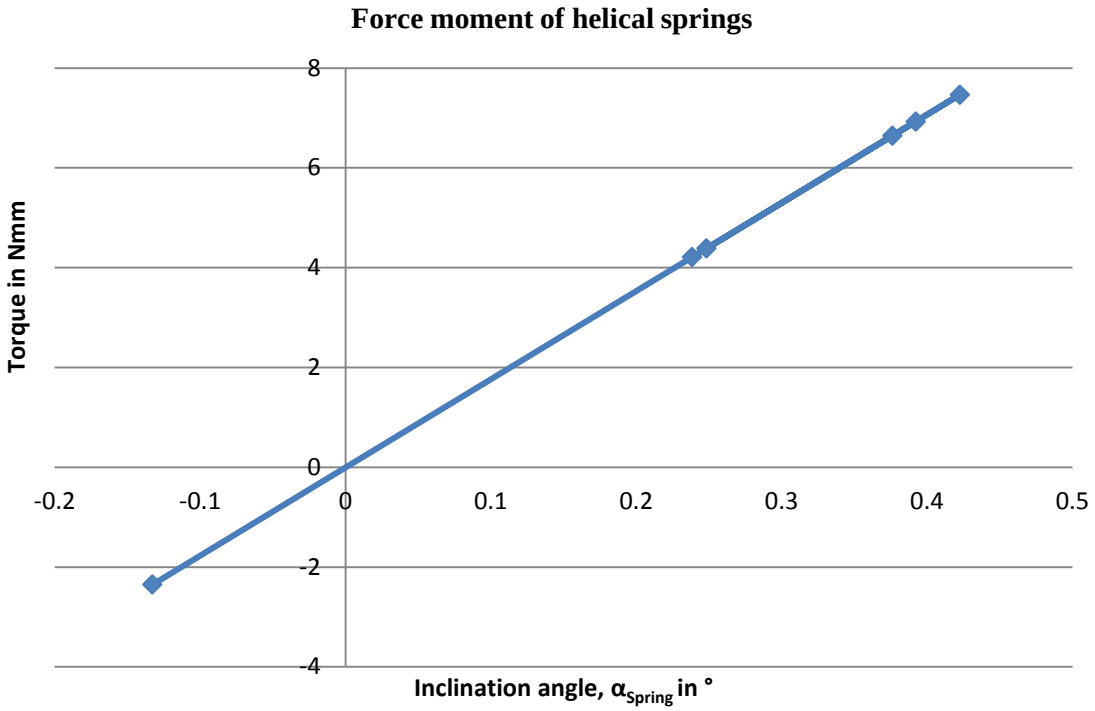

Figure 15. Moment of force exerted at the pivot joint of the abrasive holder.

After the first experiment, the prepared surfaces of the abraded abrasive blocks (the fickerts) were directly employed at the second experiment, focused on the enhancement of the surface quality of the porcelain tile.

Figure 16 shows a surface diagram from the topography measurement of the machined surface on the sample, S2. The vertical axis represents the cumulative variation of height, so that its derivative with regard to time represents the removal rate of the tile surface for each mesh number. As could be expected, such rates decrease from the coarsest abrasives to the finest ones. The smallest distance from center refers to the inner side of the machined surface. Considering that the pressure gradient operates along this axis, the farther from the centre, the smaller is the normal load acting on the tile surface. Accordingly, the lowest level was observed in the diagram part corresponding to the outermost region of the tile after being polished only with the biggest abrasive particles (#320). Furthermore, the highest material removal of 51 μm is at 35 mm distance from the tile centre and it occurred after the work of all abrasive meshes.

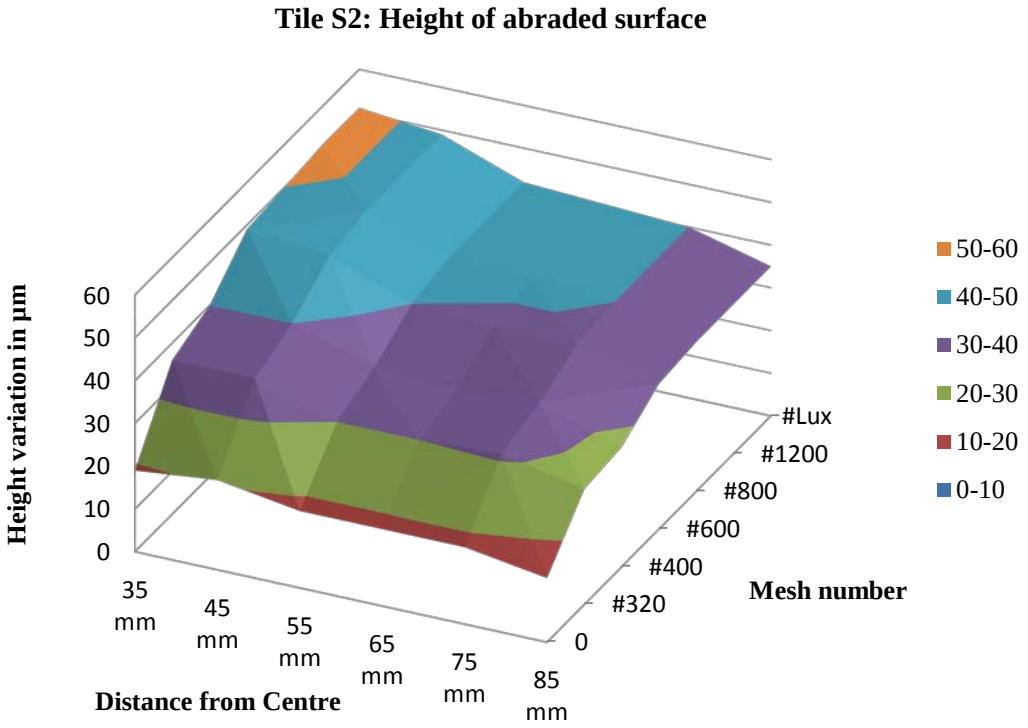

Figure 16. Height variation of machined surface measured from the centre of ceramic tile, S2.

Thus, a general trend may be recognized by obeying the Archard-type law for abrasion, also according to the equation of spring pressure given by equation (10). According to literatures, [11-12] the machining mode affects the surface quality of the machined samples. For finer grain size, a higher load is unable to force the grains to penetrate the ceramic deeper than the critical cutting depth, since the grain projection is smaller than the critical cutting depth itself. The process is therefore maintained in ductile-mode.

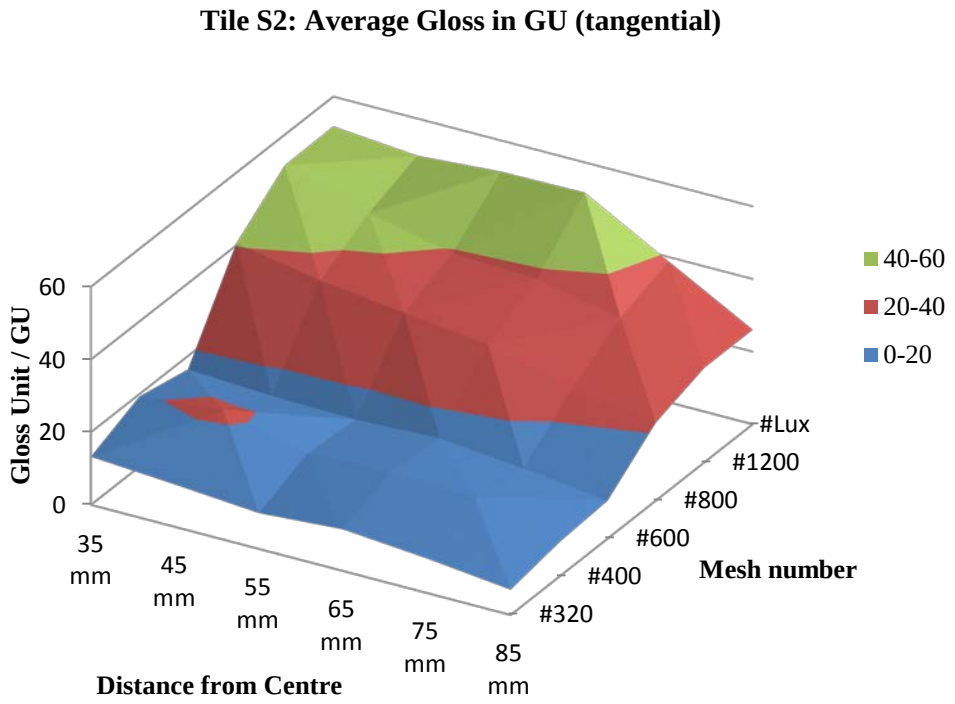

Figure 17. Gloss Unit measured in direction tangential to the tile's radius.

In figures 17 and 18, the evolution of gloss and surface roughness are presented respectively. As expected, the gloss is inversely related to the surface roughness, in the sense that a finer surface finish means a high value of gloss. Different from surface roughness however, load had a noteworthy effect on gloss. Higher loads indicate higher values of gloss [12]. The glossmeter was always aligned perpendicular to the direction of the tile's radius.

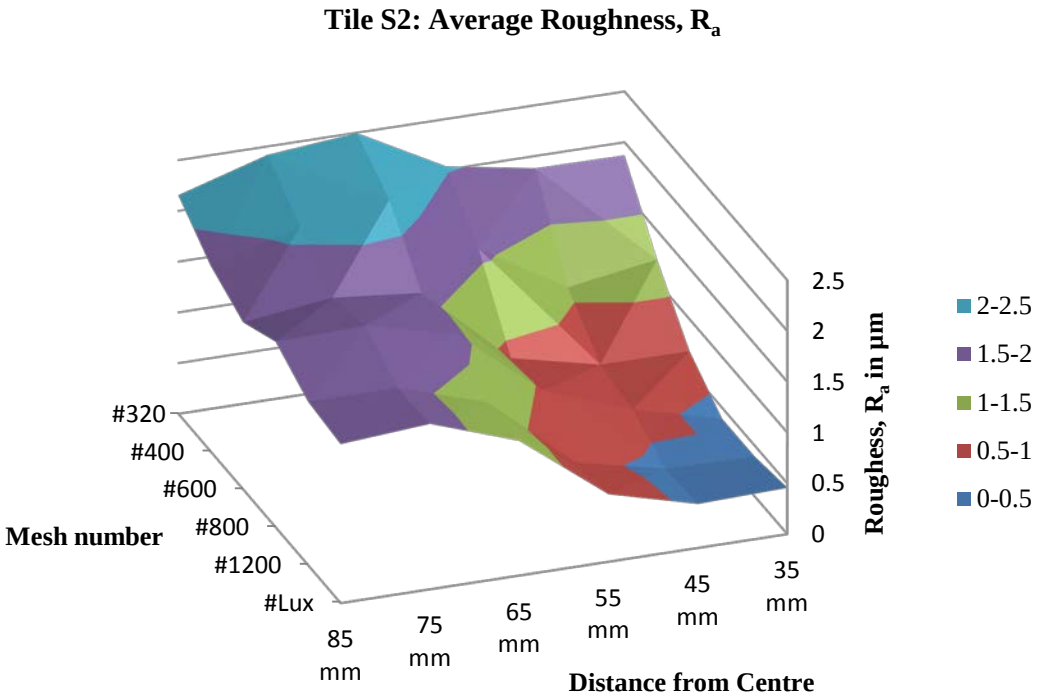

Figure 18. Average surface roughness measured from inner to outer side of the tile's machined surface.

It can be concluded from the diagrams of material removal (figure 16), gloss value (figure 17) and surface roughness (figure 18) discussed previously that, the highest gloss is found at the position where the material removed from the machined surface is the highest, subsequently provided the lowest value of surface roughness, R_a and where the highest load was exerted.

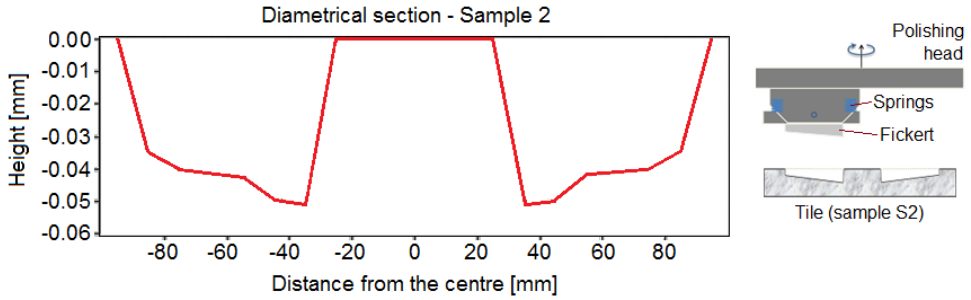

Figure 19. The abraded surface of ceramic tile S2 after polishing with increasing mesh numbers of the fickert.

In the sketch on the right side of figure 19, the worn out surface of the ceramic tiles after polishing were exaggerated for better visualization. The sketches of both tools and ceramic tiles illustrate their general trends during the polishing process. An inclined surface topography of the abrasive blocks is comparable to the inclined worn out area of the ceramic tile. However, it was found that the worn out surface of the ceramic tile is very insignificant when compared to the fickert abrasion, where $\alpha_{Abrasive} >> \alpha_{Tile}$, with the average value of α_{Tile} is always lesser than 0.01° and $\alpha_{Abrasive}$ is lesser than 1°.

As simulated elsewhere [9,13,16] and in agreement with the polishing work during polishing reported by Cantavella [8], the innermost area of the fickerts produced the highest value of glossiness where the lowest scratching speed was experienced, i.e. on the innermost region of the tile.

This work in laboratory scale revealed that, the rotation speed, the geometrical size of the polishing head, the load during polishing and the chosen kinematics are all important factors influencing the evolution of gloss during polishing. The effect of pressure and velocity gradient did affect the development of surface finish of the unglazed porcelain ceramic tiles.

This investigation on the effect of pressure gradient was studied using flat surface of the fickerts. It would be interesting to assess the effects of surface pressure on a small area or line contact between the fickerts and the ceramic tiles on the development of surface finish. The process outcomes from the current study may also be compared by polishing the ceramic tile with the same methodology without the presence of helical springs.

Finally, by solving all the equations for determining the pressure gradient occurring along the radial direction on the abrasive blocks, the values of P_{Max} and P_{Min} exerted on all the abrasive blocks during the polishing process of sample 2 are given in table 3.

Table 3. Minimum and maximum pressure distribution during the polishing process of ceramic tile, S2

Mesh number	P_N in MPa	P_{spring} in MPa	P_{max} in MPa	P_{min} in MPa
#320	0.17	0.1155	0.2855	0.0545
#400	0.17	0.0731	0.2431	0.0969
#600	0.17	0.0702	0.2402	0.0998
#800	0.17	0.1107	0.2807	0.0593
#1200	0.17	0.1244	0.2944	0.0456
#Lux	0.17	-0.0392	0.1308	0.2092

The highest pressure calculated, which was exerted on the sample, S2 during all the tests, is about 0.3 N/mm^2 and the lowest pressure is about 0.05 N/mm^2. These values represent the pressure distributed by abrasive blocks with contact surface area of 600 mm^2.

5. Conclusion

This work in laboratory scale confirmed that the scratching speed and the contact pressure are strongly related and that both are important factors influencing the evolution of the surface quality during polishing. The stabilization of the abrasive tool and the evolution of the tile surface in terms of gloss and roughness could be quantitatively evaluated using two different experimental approaches.

The findings revealed that the smallest material removal occurs at the peripheral region of the tile, where the scratching speed is higher, but the contact pressures are conversely smaller. Inward force acting towards the radial distance of the abrasive tool gives evidence to the existence of pressure gradient which is generated by the difference in scratching speed between innermost and peripheral abrasives. Such pressure gradients were experimentally measured using helicoidal springs. The values are those gradients distributed from across an area of contact of 600 mm^2 and ranging from the lowest to the maximum pressure of 0.05 N/mm^2 to 0.3 N/mm^2 respectively.

6. Acknowledgement

This work was partially supported by University Malaysia of Pahang (grant number: RDU140128), Ministry of Higher Education Malaysia and a collaboration of following entities: the Deutsche Forschungsgemeinschaft (DFG) and the Coordination for the Improvement of High Education Personnel (CAPES) in the scope of the Brazilian – German Collaborative Research Initiative on Manufacturing Technology (BRAGECRIM).

References

[1] Klocke F and König W 2005 *Fertigungsverfahren 2 - Schleifen, Honen, Läppen* 4th ed. Berlin Heidelberg: Springer (in German)
[2] Sousa F J P 2014 Polishing, *CIRP* 957-962
[3] Sánchez E, García-Ten J, Sanz V and Moreno A 2010 Porcelain tile: Almost 30 years of steady scientific-technological evolution, *Ceram. Int.* **36** 831-845
[4] Berto A M 2007 Ceramic tiles: Above and beyond traditional applications *J. Eur. Ceram. Soc.* **27** 1607-1613
[5] Sanchez E, Garcia-Ten J, Ibanez M J, Feliu C, Sanchez J, Portoles J, Soler C, Sales J, Mulet F, Gomez F J 2004 Comparative study of polished porcelain tile properties *Qualicer* **2** 449-464
[6] Hutchings I M, Adachi K, Xu Y, Sánchez E, Ibáñez M J, Quereda M F 2005 Analysis and laboratory simulation of an industrial polishing process for porcelain ceramic tiles *J. Eur. Ceram. Soc.* **25** 3151-3156
[7] Sanchez E, Ibanez M J, García-Ten J, Quereda M F, Hutchings I M, Xu Y M 2006 Porcelain tile microstructure: Implications for polished tile properties *J. Eur. Ceram. Soc* **26** 2533-2540
[8] Cantavella V, Sánchez E, Ibáñez M J, Orts M J, García-Ten J, Gozalbo A 2004 Grinding work simulation in industrial porcelain tile polishing *Key Eng. Mater.* **264 - 268** 1467-1470
[9] de S. Nascimento A S B and Sousa F J P 2014 Distribution of contact pressure over the surface of ceramic floor tiles during the polishing process *J. Eur. Ceram. Soc.* **34** 3209-3215
[10] Olenburg A, Sousa F J P, Aurich J C and Sánchez E 2013 Polishing of porcelain tiles in industrial and laboratory-scale *cfi – Ceramic Forum Inernational* **90/3** E39-E43
[11] Olenburg A, Salati M R, Sant 'Ana F and Sousa F J P 2013 Polishing process of ceramic tiles - Variation of contact pressure *Adv. Mat. Res*, **769** 124-130
[12] Hutchings I M, Xu Y, Sánchez E, Ibánez M J and Quereda M F 2005 Development of surface finish during the polishing of porcelain ceramic tiles *J. Mater. Sci. Technol.* **40** 37-42
[13] Sousa F J P, Aurich J C, Weingaertner W L and Alarcon O E 2007 Kinematics of a single abrasive particle during the industrial polishing process of porcelain stoneware tiles *J. Eur. Ceram. Soc.* **27** 3183-3190
[14] Febrotec Federn, Access (February 2014). Retrieved from Febrotec GmbH:. http://www.febrotec.de/content.php?seite=shop/produkte.php&hauptrubrik=2&details=2215
[15] Hutchings I M, Adachi K, Xu Y, Sánchez E and Ibánez M J Laboratory simulation of the industrial ceramic tile polishing process 2004 *Qualicer* **1** 19-30
[16] Sousa F J P, Weingärtner W L and Alarcon O E 2009 Computational simulation of the polishing process of porcelain stoneware tiles *Interceram* **59** 47-50